Neuron, Vol. 47, 281–293, July 21, 2005, Copyright ©2005 by Elsevier Inc. DOI 10.1016/j.neuron.2005.05.031

Do Motoneurons Encode the Noncommutativity of Ocular Rotations?

Fatema F. Ghasia and Dora E. Angelaki*
Department of Neurobiology
Washington University School of Medicine
St. Louis, Missouri 63110

Summary

As we look around, the orientation of our eyes depends on the order of the rotations that are carried out, a mathematical feature of rotatory motions known as noncommutativity. Theorists and experimentalists continue to debate how biological systems deal with this property when generating kinematically appropriate movements. Some believe that this is always done by neural commands to a simplified eye plant. Others have postulated that noncommutativity is implemented solely by the mechanical properties of the eyeball. Here we directly examined what the brain tells the muscles, by recording motoneuron activities as monkeys made eye movements. We found that vertical recti and superior/inferior oblique motoneurons, which drive sensory-generated torsional eye movements, do not modulate their firing rates according to the noncommutative-driven torsion during pursuit. We conclude that part of the solution for kinematically appropriate eye movements is found in the mechanical properties of the eyeball, although neural computations remain necessary and become increasingly important during head movements.

Introduction

When a rigid body is rotated around arbitrary axes in three dimensions, its final position depends on the order in which the rotations about the various axes are carried out (i.e, rotation A followed by rotation B is not equal to B followed by A). How a biological system, such as the eyeball, deals with this geometrical property, known as noncommutativity (Goldstein, 1980; Tweed et al., 1999), constitutes a particularly challenging problem that has caused controversy and considerable debate (for recent reviews see Angelaki and Hess, 2004; Crawford et al., 2003). This issue has been addressed mostly during saccades and smooth pursuit, both of which are visually guided eye movements driven by two-dimensional (i.e., horizontal, vertical) retinal information. Three-dimensional eye orientation during saccades and pursuit is thus confined to a horizontal/vertical plane, referred to as Listing's plane (Ferman et al., 1987; Haslwanter et al., 1991; Tweed and Vilis, 1987, 1990; Tweed et al., 1992). Because rotational mathematics do not follow simple (commutative) vector algebra, an unintuitive paradox exists in which eye *positions* in Listing's plane have zero torsion, but the eye movements required to achieve these positions must have *velocities* with a nonzero torsional component (Haslwanter, 1995, 2002; Tweed and Vilis, 1987, 1990). Thus, when eye movements are made from eccentric positions, the angular velocity axis of the eye does not remain confined to Listing's plane but deviates in the same direction as gaze by approximately half as much (*half-angle rule*; Figure 1A; see also Tweed and Vilis, 1987, 1990).

How this torsional eye velocity, which is necessary to keep eye position in Listing's plane, is generated *in the absence of relevant sensory drive* has been in the center of the controversy. Tweed and Vilis (1987, 1990) were the first to address this problem in modern times (see also von Helmholtz, 1867; Westheimer, 1957). Under the prevailing assumption of the late 1980s that the muscle pulling directions remain independent of eye position, Tweed and Vilis proposed that nonlinear (i.e., multiplicative) mathematical operations exist within the neural network implementing the velocity-to-position neural integrator (Cannon and Robinson, 1987; Skavenski and Robinson, 1973), such that motoneuron firing rates carry this eye position-dependent torsional component (Figure 1B, scheme 1). More recently, however, a contrasting view to such a "neural" solution was proposed. According to this alternative "mechanical" hypothesis, Demer and colleagues (Demer et al., 1995; Miller et al., 1993) postulated that mobile, soft-tissue sheaths (pulleys) in the orbit can influence the direction of action of the extraocular muscles, possibly allowing for a position-dependent shift in the rotation axis of the eye, despite identical motoneuron commands (Figure 1B, schemes 2a and 2b). This proposal was subsequently quantified by model simulations showing that appropriately placed pulleys may simplify the brain's work in dealing with noncommutativity (Quaia and Optican, 1998; Raphan, 1998). Magnetic resonance imaging of rectus muscle paths has since shown that the pulley arrangement is consistent with an oculomotor plant that could implement the position dependence of eye velocity in Figure 1A (Demer et al., 2000, 2003; Kono et al., 2002).

This conjecture, based primarily on histological and fMRI results by Demer and colleagues, remains controversial and often challenged by other behavioral, computational, and physiological studies (Angelaki, 2003; Dimitrova et al., 2003; Misslich and Tweed, 2001; for recent reviews see Angelaki and Hess, 2004; Crawford et al., 2003). A definitive and necessary experiment to distinguish between a potentially *exclusively neural* and an *at least partly mechanical* solution to the problem of noncommutativity is to examine what the brain tells the muscles, e.g., to characterize the physiological properties of extraocular motoneurons. If noncommutative-driven torsion is exclusively neurally computed (Figure 1B, scheme 1), this signal should always be carried by vertical (i.e., superior/inferior oblique and superior/inferior rectus) motoneurons. Alternatively, if the half-angle rule is mechanically implemented (Figure 1B, schemes 2a and 2b), no torsional command to move the eye should be found in motoneuron activities during horizontal and vertical smooth pursuit eye movements. Our

*Correspondence: angelaki@pcg.wustl.edu

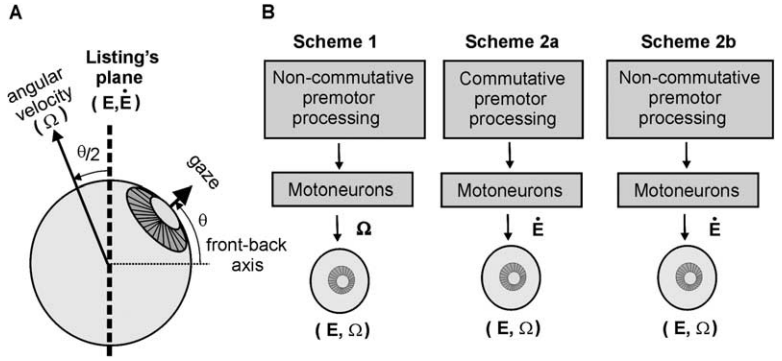

Figure 1. Illustration of the Problem and Hypotheses

(A) Schematic illustration of the half-angle rule (side view). The mathematical relationship between eye position, E, the derivative of eye position, $\dot{E} = dE/dt$, and angular velocity, Ω, is: $E = 2\dot{E}/\Omega$ (when expressed as quaternions; Goldstein, 1980; Tweed and Vilis, 1987). During eccentric gaze, eye movements that keep E and $\dot{E}$ in Listing's plane (vertical thick dashed line) must rotate the eyeball with an angular velocity, Ω, that tilts out of Listing's plane by half the angle ($\theta/2$) of the deviation in gaze (θ). This occurs because an eye position-dependent torsional component (defined here as the eye rotation about the front-back axis) is "added" to eye velocity during horizontal eye movements (rotation about the vertical axis). For simplicity, Listing's plane has been drawn perpendicular to the front-back axis.

(B) Three alternative schemes for the control of eye orientation. Scheme 1: the original (*neural*) hypothesis of Tweed and Vilis (1987) assumes that the pulling directions of the muscles remain head fixed and that motoneurons encode angular velocity, Ω, rather than $\dot{E}$. Schemes 2a and 2b: the *mechanical* hypothesis assumes that motoneurons encode $\dot{E}$, from which angular velocity, Ω, is constructed by the eye plant itself. Variants *a* and *b* only differ in the premotor neuron properties. Scheme 2a represents an extreme view, according to which the brain need not be aware of noncommutative mathematics (Raphan, 1998). Scheme 2b illustrates a mathematically and experimentally more viable solution, where noncommutative computations continue to be necessary for motor planning of eye movements (Smith and Crawford, 1998; Tweed et al., 1994, 1999). The present experiments aim to address whether motoneurons encode Ω or $\dot{E}$ and do not directly distinguish between schemes 2a and 2b (see Discussion).

results demonstrate that motoneurons do not carry the eye position dependence of eye velocity necessary to generate smooth pursuit eye movements in Listing's plane, supporting the hypothesis that part of the solution for kinematically appropriate eye movements is found in the mechanical properties of the eyeball.

Results

We recorded neural activities from 99 neurons that were located either within the oculomotor (OC, III) and trochlear (TR, IV) motor nuclei or were fibers within the OC/TR rootlets. The majority were vertical motoneurons, innervating the superior/inferior recti and superior/inferior oblique muscles. Of these vertical motoneurons, 22 were identified as TR nerve fibers, 16 as vertical OC fibers, and 40 were vertical cells in the TR/OC nuclei. In addition, activities from 21 medial rectus (horizontal) motoneurons were also recorded for comparison. Of these, 9 were fibers recorded in the OC nerve rootlets, while the remaining 12 were cells recorded in the OC nuclei. All neurons included in this study were isolated within the center of the respective nuclei. In addition, only neurons and fibers with clear burst-tonic activities, including a strong saccadic sensitivity, were included in the sample. Unless a specific difference needs to be highlighted, we refer to both cell body and fiber recordings as "motoneurons," "cells," or "neurons" in the following presentation.

To compare between the predictions of an exclusively neural (abbreviated here as simply "neural") and an at least partly mechanical (abbreviated here as simply "mechanical") hypothesis (Figure 1B, scheme 1 versus schemes 2a and 2b), we used two different types of sensory stimuli: (1) yaw, pitch, and roll head and body rotations, generating horizontal, vertical, and torsional vestibulo-ocular reflexes (VOR), respectively; and (2) horizontal and vertical smooth pursuit eye movements. With the former (head rotation) stimuli, the three-dimensional eye movement is uniquely specified by the sensory drive. Accordingly, motoneurons are expected to carry the appropriate motor drive to generate horizontal, vertical, and torsional eye velocities during yaw, pitch, and roll VOR. Thus, we refer to the torsional eye movements elicited during roll head rotation as *sensory-driven torsion*. In contrast, the latter (smooth pursuit) stimulus constitutes a two-dimensional retinal signal, where only the horizontal and vertical components of eye velocity are directly driven by the sensory stimulus. Thus, the torsional eye velocity necessary for the half-angle rule is not sensory driven, but a direct result of noncommutativity. Whether motoneurons carry the appropriate motor drive to generate this *noncommutative-driven torsion* is fundamental to the predictions of the neural and mechanical hypotheses.

Vertical motoneurons have oblique on-directions and drive both vertical and torsional eye movements, whereas the on-direction of horizontal motoneurons is almost purely horizontal (Suzuki et al., 1999). Thus, if the noncommutative-driven torsion is neurally generated (neural hypothesis), the firing rates of *all* vertical (but not horizontal) motoneurons should change proportionally to both sensory-driven and noncommutative-driven torsion. In contrast, the mechanical hypothesis predicts no such consistent correlation between firing rates and noncommutative-driven torsion, because the latter is simply due to eye position-dependent changes in the pulling direction of the rectus muscles. In a more mathematically appropriate terminology, the neural and mechanical hypotheses predict that motoneurons encode angular velocity and derivative of eye position (Figure 1B, schemes 1 versus 2a and 2b), respectively. With these predictions in mind, we first briefly show that vertical motoneurons modulate during roll head movements (eliciting sensory-driven torsion), before examining their properties during horizontal and vertical

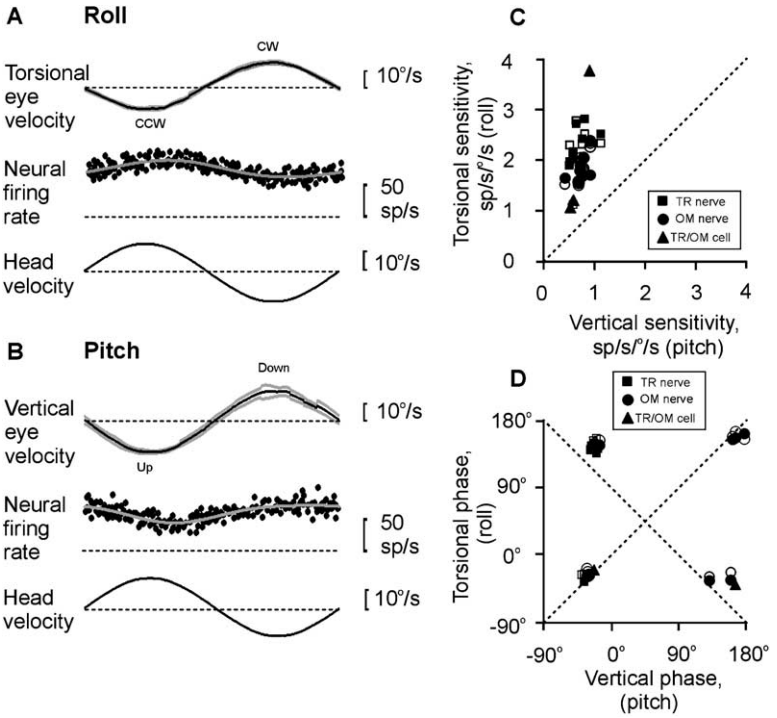

Figure 2. Motoneuron Responses during Roll and Pitch Rotations of the Head

(A and B) Modulation of a trochlear nerve fiber (middle traces) and mean (±SD, gray lines) eye velocity during roll (A) and pitch (B) head movements. The solid gray line superimposed on the instantaneous neural firing rate plot illustrates the best-fit sinusoid (see Experimental Procedures).

(C and D) Torsional eye velocity sensitivity (computed as peak cell modulation divided by peak torsional eye velocity during 2 Hz roll head oscillations) and phase plotted as a function of the respective modulation during pitch head movements (filled symbols, complete darkness; open symbols, central target fixation). Response phases close to 0° illustrate neural responses in phase with clockwise (roll) or downward (pitch) eye velocity. Response phases close to 180° illustrate neural responses in phase with counterclockwise (roll) or upward (pitch) eye velocity. Data are shown separately for trochlear (TR) nerve fibers (squares), oculomotor (OM) nerve fibers (circles), and neurons in the TR/OC nuclei (triangles). n = 24.

smooth pursuit eye movements (eliciting noncommutative-driven torsion).

Sensory-Driven Torsion: Motoneuron Responses during Roll Head Movements

As expected from their on-directions, all vertical motoneurons modulated during both roll and pitch head movements, generating torsional and vertical eye movements, respectively. Figures 2A and 2B illustrate the responses of a TR nerve fiber during 2 Hz roll and pitch rotations. This fiber increased its firing rate with negative (counterclockwise from the animal's viewpoint) torsional eye velocity during clockwise (positive) roll rotation and downward (positive) eye velocity during upward pitch rotation. Depending on their on-direction, vertical motoneurons increased their firing rates with either positive or negative ocular torsion, with a peak response modulation that was as large or larger than the respective modulation during pitch head movements of equal amplitude.

The pitch VOR gain was higher than the roll VOR gain, with peak vertical and torsional eye velocity averaging 17.2 ± 0.6°/s and 9.4 ± 1.4°/s during 2 Hz pitch and roll head movements, respectively. Thus, when expressed relative to the motor output (eye velocity), all vertical motoneurons had higher sensitivities to torsional than vertical eye velocity, as illustrated in Figure 2C. The neural modulation phase was similar for torsional (roll) and vertical (pitch) eye movements, as illustrated in Figure 2D (data points falling along the diagonal, dotted lines; paired t test, $p >> 0.05$). Because of their strong modulation during roll head movements generating sensory-driven torsion, the neural hypothesis would predict that all vertical motoneurons should also change their firing rates in proportion to the noncommutative-driven torsion during pursuit eye movements.

Noncommutative-Driven Torsion: Motoneuron Responses during Horizontal and Vertical Pursuit Eye Movements

This type of torsional eye movement has been illustrated, along with the responses from a TR nerve fiber, in Figure 3. During horizontal pursuit at zero vertical eccentricity (central target), the animal pursued the target with an almost purely horizontal eye velocity (Figure 3A, top middle traces). In contrast, during horizontal pursuit in vertically eccentric positions, eye velocity had both horizontal and torsional components, the latter being opposite in direction for up versus down targets (Figure 3A). A similar observation was also made during vertical pursuit for left and right targets (Figure 3B). When eye velocity was plotted in head coordinates (see insets; A: side view; B: top view), eye velocity tilted in the same direction as gaze, by approximately half as much (accounting for the "half-angle rule"; Figure 1A). The ratios of peak torsional versus peak horizontal (Figure 4A) or vertical (Figure 4B) eye velocity, which change monotonically with eye position (as quantified by linear regression, solid lines), are roughly proportional to the tilt angle of eye velocity (Figure 4A,B, right axis). The slopes of these regressions were remarkably similar for the three animals and for horizontal versus vertical pursuit, averaging 0.01 ± 0.001 deg^{-1} (corresponding to an eye velocity tilt angle slope of 0.60 ± 0.07, which is only slightly larger than the 0.5 slope expected from the half-angle rule; see also Angelaki et al., 2003).

As summarized in the Introduction, this torsional

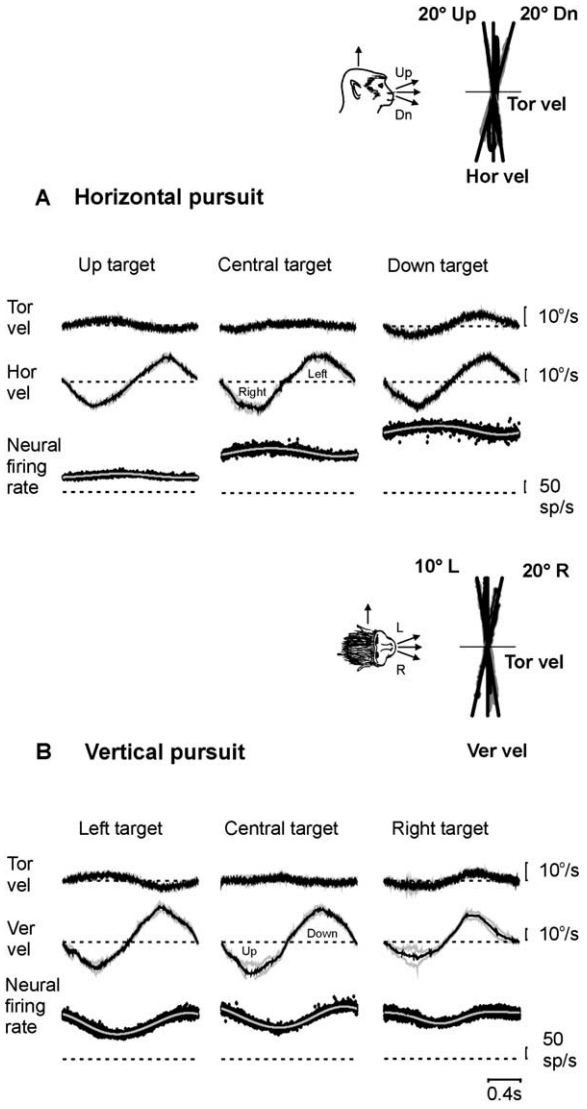

Figure 3. Motoneuron Responses during Horizontal and Vertical Smooth Pursuit Eye Movements

Eye velocity and neural responses from a trochlear nerve fiber during (A) horizontal and (B) vertical pursuit of targets at different eccentricities. From left to right, data shown are for targets moving horizontally at vertical eccentricities of 20° Up, center, and 20° Down (A) and for targets moving vertically at horizontal eccentricities of 10° left (L), center, and 20° right (R) (B). From top to bottom, traces illustrate mean torsional eye velocity and mean horizontal (A) or mean vertical (B) eye velocity (±SD, gray lines). Bottom traces illustrate neural firing rate, with the superimposed sinusoidal fit (gray lines). Notice that, as typical of all vertical motoneurons, mean firing rates increased when looking eccentrically in the cell's on-direction (down). However, it is the peak-to-trough firing rate modulation that is of interest in these comparisons. Insets on the top illustrate mean eye velocity plotted in head coordinates (see monkey's head drawing). Data are shown in gray, with superimposed black solid lines illustrating linear regression (for clarity only shown for eccentric targets).

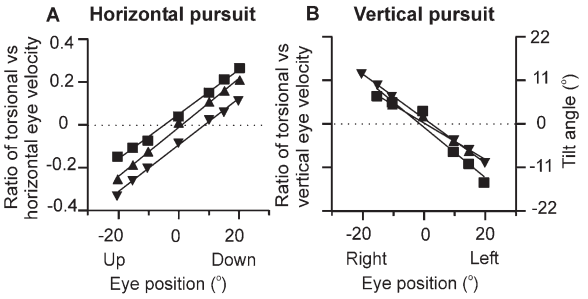

Figure 4. Noncommutative-Driven Torsion

(A and B) Ratio of peak torsional versus horizontal (A) or vertical (B) eye velocity (left axis) or the respective tilt angle of eye velocity (right axis), plotted as a function of mean vertical and horizontal eye position, respectively. Because of the definition of positive torsional, vertical, and horizontal eye movements in this study, these ratios increase with vertical eye position during horizontal pursuit (A) and decrease with horizontal eye position during vertical pursuit (B). Different symbols illustrate data from the three different animals. Solid lines illustrate linear regressions.

component of eye velocity is necessary to keep eye position in Listing's plane (Haslwanter et al., 1991; Tweed and Vilis, 1987, 1990; Tweed et al., 1992). Unlike the sensory-driven torsion generated during roll head movements, the torsional eye velocity elicited during horizontal and vertical smooth pursuit (Angelaki et al., 2003; Tweed et al., 1992) is not in response to a sensory stimulus, but reflects the rather unintuitive consequences of the noncommutative mathematics of rotations. According to the mechanical hypothesis, although vertical motoneurons change their firing rates appropriately to drive torsion during roll head movements (Figure 2), they should not systematically change their activity to reflect the added torsional velocity during eccentric pursuit. In contrast, the neural hypothesis predicts that all vertical motoneurons would exhibit the same sensitivity to this noncommutative-driven torsion as they do for the roll head movement-driven torsion. As a result, their firing rates should systematically change as the ratio of torsional versus horizontal or vertical velocity changes at different ocular eccentricities (e.g., Figure 4).

Do vertical motoneurons change their firing rates to account for the noncommutative-driven torsion? Figure 3 illustrates the vertical and horizontal pursuit responses of a typical TR nerve fiber, whose firing rate changes could be consistent with the predictions of the neural hypothesis. To appreciate this, consider that the fiber's vertical and torsional on-directions are positive (downward) and negative (ccw), respectively. Thus, peak neural firing rate increased for down eye movements (Figure 3B). If it also increased with negative ccw torsion, the two components of firing rate would add for left targets and subtract for right targets, resulting in a vertical pursuit modulation that changes with horizontal eye position. Indeed, neural "gains," defined as the ratio of peak-to-trough cell modulation (computed from sinusoidal fits; see Experimental Procedures) over peak-to-trough vertical eye velocity were 2.11 sp/s/°/s (left target), 1.94 sp/s/°/s (central target), and 1.79 sp/s/°/s (right target) (Figure 3B).

The on-direction of vertical motoneurons also includes a small horizontal component (e.g., Suzuki et al.,

1999), as illustrated by the right eye movement preference for the TR fiber of Figure 3A. The same reasoning can also be applied here to illustrate that, should this fiber carry a motor command for the noncommutative-driven torsion, its peak-to-trough modulation would be highest for down targets and lowest for left targets. Indeed, this motoneuron's gain was larger for down compared to up targets (0.97 sp/s/°/s versus 0.52 sp/s/°/s, respectively).

Neural response gain and phase from 18 trochlear nerve fibers have been illustrated in Figures 5A and 5B. Some neurons changed their peak firing rates with eye position, as would be expected from the neural hypothesis, others did not (black symbols and lines, $p < 0.05$; gray symbols and lines, $p > 0.05$; linear regression analysis). Figure 5C illustrates the expected dependence (Equations 1a and 1b in Experimental Procedures) of hypothetical motoneurons with a horizontal pursuit gain of 0.5 sp/s/°/s and vertical/torsional pursuit gains of 2 sp/s/°/s. The sign of the expected dependence of motoneuron firing rates on eye position depends on their respective on-directions, as summarized in Table 1 (see Experimental Procedures). The slope signs for horizontal and vertical pursuit should be opposite for left/down and right/up on-directions, and the same for left/up and right/down on-directions. Thus, to quantify the dependence of firing rates on eye position, we simultaneously fitted the horizontal and vertical pursuit gains as a function of the respective vertical and horizontal eye position for each cell using first-order polynomials, where the neural gain slopes were constrained to be of similar or opposite signs for horizontal and vertical pursuit, depending on the cell's horizontal and vertical on-directions (Table 1).

The steepness (slope) of this relationship depends on two factors (see Equation 1a in Experimental Procedures): (1) the ratio of torsional to vertical or horizontal eye velocity, which, as summarized above, was similar for all three animals (Figures 4A and 4B); and (2) the neuron's sensitivity to torsional eye velocity. The neural hypothesis assumes that motoneurons will be equally sensitive to sensory-driven and noncommutative-driven torsion. Thus, the best way to estimate the latter would be from the respective neuron's response to roll rotation. However, not all motoneurons were tested with roll head movements. Thus, to compute a prediction of how much neural firing rates should change as a function of eye position for *all* motoneurons tested during pursuit, their torsional velocity sensitivity was first approximated to be equal to the cell's vertical sensitivity (i.e., the neuron's vertical pursuit gain at zero horizontal eccentricity). Such an approximation would be consistent with the roughly equal torsional and vertical on-directions of vertical motoneurons during static fixations (Suzuki et al., 1999). Yet, because motoneuron torsional eye velocity sensitivities were typically larger than vertical sensitivities (Figure 2D), the slopes predicted using this approximation most likely represent a conservative *lower estimate* (i.e., an underestimation) of the expected dependence.

The predicted versus actual slopes of the linear dependence of cell firing rates on eye position have been summarized in Figure 6A. For the majority of motoneurons, the predicted slope was larger than the one actually observed, and this difference was statistically significant (paired t test, $p << 0.001$). More than one-third (22/59, 37%) of the cells had slopes that were lower than 25% of the respective predictions. In contrast, only 12% (7/59) of the cells had slopes larger than 75% of the predicted values. These proportions were equally split between TR and OC nerve fibers and neurons within the motor nuclei (Figure 6A; black squares, circles, and triangles, respectively). We searched for differences between these two populations in terms of

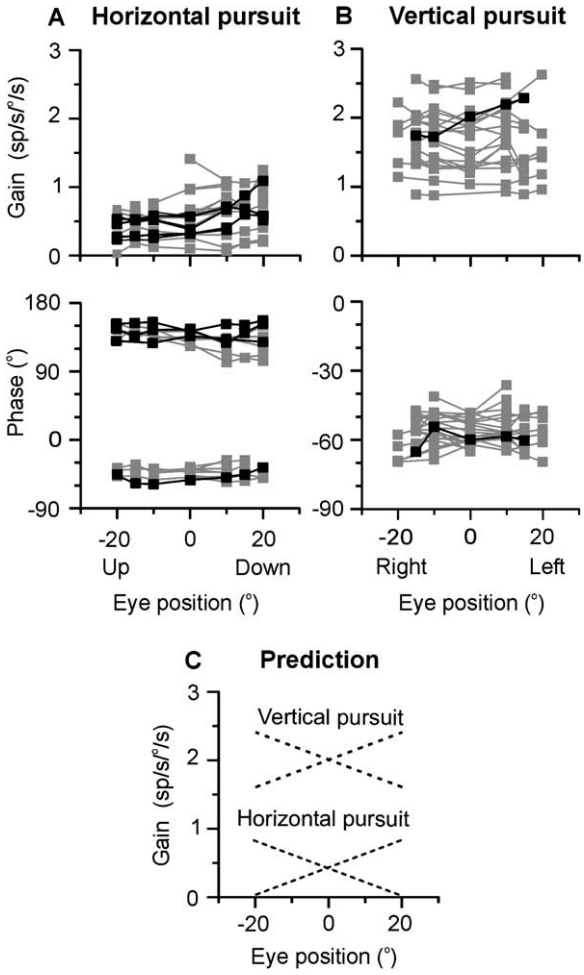

Figure 5. Dependence of Neural Firing Rates on Eye Position

(A and B) Eye position dependence of the gain of 18 TR nerve fibers during horizontal (A) and vertical (B) pursuit. Fibers with a statistically significant ($p < 0.05$) gain change as a function of eye position (based on linear regressions; see Experimental Procedures) are shown with black symbols and lines, whereas the rest of the fibers (with $p > 0.05$) are shown in gray. The two groups whose horizontal pursuit phase differs 180° correspond to TR fibers with leftward versus rightward horizontal preferred directions (Suzuki et al., 1999).

(C) Predicted eye position dependence of a hypothetical vertical motoneuron with vertical/torsional sensitivities of 2 sp/s per °/s and a horizontal sensitivity of 0.5 sp/s per °/s. Notice that, because this hypothetical motoneuron has positive horizontal, vertical, and torsional on-directions, the predicted dependence on eye position should be opposite for vertical and horizontal pursuit (for a complete set of predictions, see Table 1).

Table 1. Expected Sign of the Eye Position Dependence of Motoneurons during Horizontal and Vertical Pursuit as a Function of Their On-Directions—Neural Hypothesis

Motoneurons On-Directions			Eye Position-Dependent Slopes	
Horizontal	Vertical	Torsional	Horizontal Pursuit	Vertical Pursuit
Left	down	positive	+	–
Left	down	negative	–	+
Right	up	positive	–	+
Right	up	negative	+	–
Left	up	positive	+	+
Left	up	negative	–	–
Right	down	positive	–	–
Right	down	negative	+	+

pursuit and VOR gain and phase, as well as static eye position and saccadic sensitivities, but found that none of these properties differed significantly for cells with small and large eye position slopes ($p > 0.05$). The very small percentage of vertical motoneurons with potentially appropriate slope magnitude does not support the predictions of the neural hypothesis, according to which *all* vertical motoneurons (which drive sensory-driven torsion) should also change their firing rates according to the noncommutative-driven torsion.

Comparison of Motoneuron Firing Rates during Sensory-Driven and Noncommutative-Driven Torsion

Eighteen motoneurons were tested during both horizontal/vertical pursuit and roll head movements (Figure 2). For these neurons, a more accurate prediction of expected slope could be made, since the torsional eye velocity sensitivity of the cell was directly measured during the 2 Hz roll oscillations. Figure 6B compares the actual with the predicted slopes for motoneurons whose sensitivities to torsional eye velocity were directly estimated during 2 Hz roll head movements. For these comparisons, because the cell's torsional on-direction was also known (i.e., the cell encoded either positive or negative torsion during roll head movements), the sign of the expected slopes (i.e., whether it was predicted to increase or decrease as a function of eye position) could also be predicted. As illustrated in Figure 6B, the actual motoneuron slopes were typically *smaller* than those predicted from the cells' sensitivities to sensory-driven torsion (paired t test, $p << 0.001$). Furthermore, the actual changes in neural firing rates were often in the *incorrect direction* from that expected if the cell's on-directions for sensory-driven and noncommutative-driven torsion were the same (shaded quadrants in Figure 6B). Therefore, the eye position dependence of many vertical motoneuron firing rates is not only much smaller in magnitude, but also often in the wrong direction to be consistent with the predictions of the neural hypothesis.

Control Experiments

To further illustrate that the predictions of the neural hypothesis were not supported by the data, we performed two control experiments. First, we also recorded from 21 medial rectus motoneurons during horizontal and vertical pursuit at different vertical and horizontal eccentricities, respectively. Because their on-direction does not have a torsional component (Suzuki et al., 1999), the neural hypothesis predicts *no* dependence of medial rectus motoneuron firing rates on eye position. To directly compare the relative slopes of horizontal and vertical motoneurons (and since no "prediction" could be made for the former), we also quantified the dependence of firing rates on eye position using linear regression, separately for horizontal and vertical pursuit. These values, now plotted on a cell-by-cell basis as the respective slopes during vertical pursuit versus the corresponding slopes during horizontal pursuit have been illustrated in Figures 7A and 7B. The resulting eye position slopes and p values of medial rectus motoneuron firing rates (Figure 7B, gray diamonds) were not different from those of vertical motoneurons (Figure 7A, black squares, circles, and triangles, respectively) (t test, $p >> 0.05$). Thus, whatever the reason for the small eye position dependence of some cells (see Discussion), the fact that it is of similar magnitude for both vertical and horizontal motoneurons does not support the predictions of the neural hypothesis.

Second, for seven vertical motoneurons, we also recorded neural activities while varying eye position in

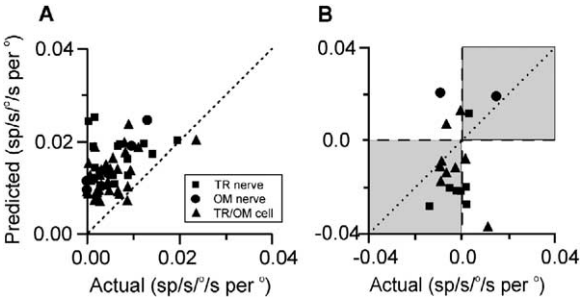

Figure 6. Comparison of Predicted versus Actual Vertical Motoneuron Firing Rate Slopes of Neural Response Gain during Vertical Pursuit as a Function of Eye Position

The illustrated slopes correspond to simultaneous fits of horizontal and vertical pursuit gains (see Experimental Procedures). The predictions were computed with torsional sensitivity being either (A) approximated to be equal to the cell's vertical response sensitivity or (B) directly measured during roll head movements. Shaded areas in (B) illustrate the quadrants where predicted and actual slopes were of the same sign. Different symbols identify TR nerve fibers (squares), OC nerve fibers (circles), and cells recorded in the TR/OC nuclei (triangles). Dotted line illustrates the unity-slope line. n = 59 (A) or 18 (B).

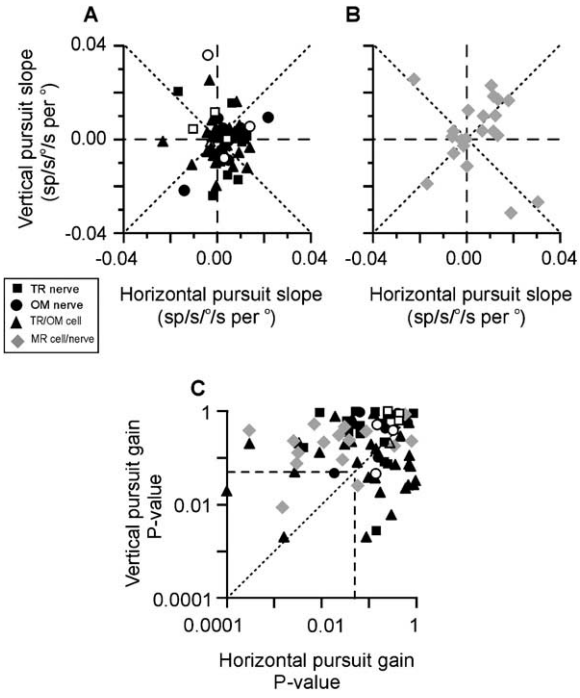

Figure 7. Comparison of the Eye Position Dependence for Vertical and Horizontal Motoneurons

(A and B) Summary of vertical (n = 60) (A) and horizontal (n = 21) (B) motoneuron slopes when horizontal and vertical pursuit data were fitted separately. (C) Corresponding p values for the fits. Vertical motoneurons include TR nerve (squares), OC nerve (circles), and TR/OC cells (triangles). Horizontal motoneurons are from the medial rectus (MR; gray diamonds). Open symbols illustrate vertical motoneurons tested at different horizontal eye positions during horizontal pursuit and vertical eye positions during vertical pursuit (conditions that do not elicit noncommutative-driven torsion). Dotted lines illustrate the unity-slope lines. Dashed lines illustrate either the zero baselines (A and B) or the 0.05 level of significance (C).

the same direction as pursuit (i.e., by varying vertical eye position during vertical pursuit and horizontal eye position during horizontal pursuit), a condition that evokes no noncommutative-driven torsion. Under these conditions, because the neural hypothesis predicts changes in motoneuron firing rates as a function of eye position *only* when the latter is accompanied by the generation of torsional eye velocity, motoneuron slopes should be negligible or at least smaller than those when the noncommutative torsion is present. Once again, we found this prediction not to be supported by the data. The slopes of vertical motoneuron firing rates as a function of eye position in the conditions where no noncommutative-driven torsion was generated were similar to those when a noncommutative-driven torsion was evoked (Figure 7A, open versus filled black symbols, paired t test, $p >> 0.05$). The corresponding p values of the regression have been illustrated in Figure 7C. These results suggest that similar eye position-dependent changes were present in both horizontal and vertical motoneuron firing rates, either in the presence or absence of noncommutative-driven torsion. Thus, because changes in motoneurons firing rates with eye position did not correlate with noncommutative-driven torsion, we conclude that the small changes in some motoneuron firing rates with eye position are likely due to factors other than the noncommutative-driven torsion (see Discussion).

Noncommutative-Driven Torsion: Eye Position Dependence of Yaw and Pitch VOR

A similar analysis to that described above for horizontal and vertical pursuit was also done on cell responses during yaw and pitch rotations. The VOR does not follow the half-angle rule, but shows a much smaller dependence on eye position (Angelaki et al., 2003; Crawford and Vilis, 1991; Misslich et al., 1994; Misslich and Hess, 2000). The respective eye velocity ratios and tilt angles for yaw and pitch VOR in these animals have been illustrated in Figure 8. The dependence on eye position was similar, but smaller for the VOR than for pursuit eye movements (compare Figures 8A and 8B with Figures 4C and 4D), with VOR slopes averaging 0.005 ± 0.0008 deg^{-1} (corresponding to an eye velocity tilt angle slope of 0.29 ± 0.04; often referred to as the "quarter-angle rule"; Misslich et al., 1994).

Given the smaller torsional eye velocities generated during the VOR, if the noncommutative-driven torsion is encoded by the firing rates of vertical motoneurons, cell activities during the VOR should be characterized by smaller eye position slopes that those during pursuit. Once again, data did not support this prediction, as illustrated in Figures 8C and 8D, which plot the respective slopes during the yaw and pitch VOR with those during horizontal and vertical pursuit, respectively. The eye position slopes of vertical motoneurons were not different for yaw VOR versus horizontal pursuit and pitch VOR versus vertical pursuit (paired t test, $p >> 0.05$).

Discussion

Neural versus Mechanical Solution for Noncommutativity during Smooth Pursuit Eye Movements

We have directly tested whether motoneurons with vertical on-directions change their firing rates during pursuit eye movements, as expected according to a purely neural solution to the problem of noncommutativity (Figure 1B, scheme 1). We found that although they carry the torsional drive during roll movements of the head, vertical motoneurons do not consistently change their firing rates during horizontal and vertical pursuit eye movements from eccentric positions, as would have been expected if they provided the motor drive for the noncommutative-driven torsion. Four different observations contributed to this conclusion. First, changes in motoneuron firing rates with eye position were typically smaller and often in the incorrect direction from those expected if motoneurons provided the same motor drive for sensory-driven and noncommutative-driven torsion. Second, small firing rate changes were also seen when eye position changed in the same (rather than orthogonal) direction to pursuit, a condition that does not generate noncommutative-driven torsion (Tweed and Vilis, 1987, 1990; Tweed et al., 1992). Third,

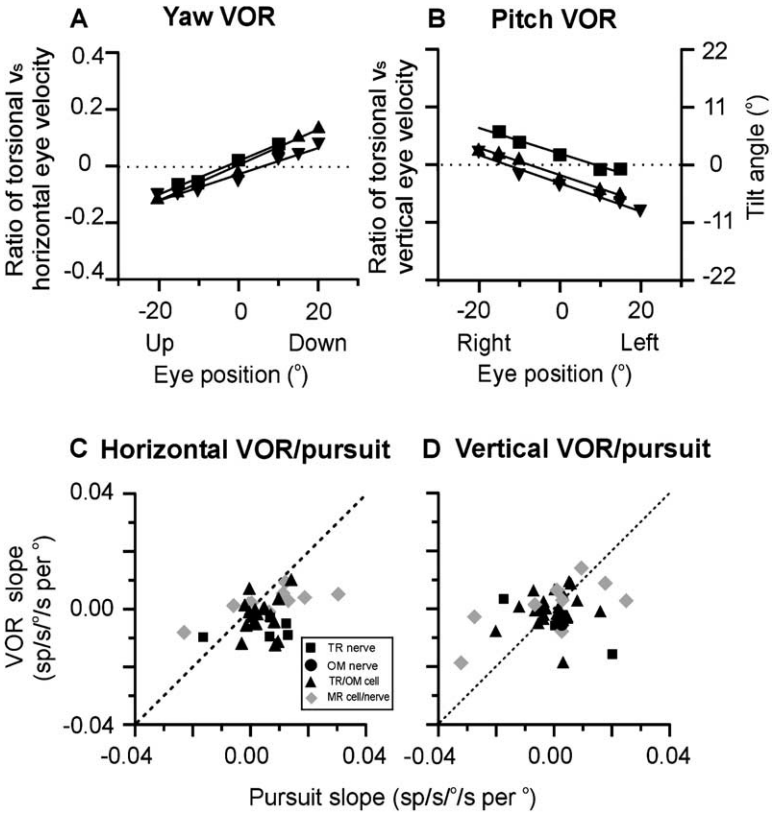

Figure 8. Comparison of VOR and Pursuit Slopes

(A and B) Ratio of peak torsional versus peak horizontal (A) or vertical (B) eye velocity (left legend) or the respective tilt angle of eye velocity (right legend), plotted as a function of mean vertical and horizontal eye position, respectively. Because of the definition of positive torsional, vertical, and horizontal eye movements in this study, these ratios increase with vertical eye position during yaw VOR (A) and decrease with horizontal eye position during pitch VOR (B). Different symbols illustrate data from the three different animals. (C and D) Summary of neural slopes, computed using linear regression separately during horizontal (C) and vertical (D) VOR/pursuit. Data are from both vertical motoneurons (TR nerve, squares; OC nerve, circles; TR/OC cells, triangles) and medial rectus (MR) motoneurons (gray diamonds). n = 34 (A) or 38 (B).

medial rectus motoneurons, with purely horizontal on-directions, also exhibited similar behaviors as vertical motoneurons. Because there is no torsional component in the on-direction of medial rectus motoneurons (Suzuki et al., 1999), the neural hypothesis predicts an eye position-dependent change in the firing rates of vertical, but not horizontal, motoneurons.

As experimental observations do not agree with these predictions, we suggest that the occasional small eye position dependence, seen in either vertical or horizontal motoneuron firing, is most likely unrelated to noncommutative-driven torsion and probably due to other complexities of the eye plant (Goldberg et al., 1998; Goldberg and Shall, 1999; Miller and Robins, 1992; Porrill et al., 2000; Quaia and Optican, 2003). The small eye position dependence could also be due to the small (~0.7°; see Experimental Procedures) vergence angle changes for central versus eccentric targets (Mays et al., 1991). Because of their very characteristic burst-tonic activities and strong saccadic sensitivities, as well as their location within the center of the OC/TR nuclei, the motoneuron populations studied here most likely innervate twitch nerve fibers, which are important for the generation of eye rotations (Buttner-Ennever and Horn, 2002; Buttner-Ennever et al., 2001). It is less clear, though, whether the recorded population innervated the global or orbital layers, as their physiological and anatomical landmarks remain unknown.

The fourth and final result against the neural hypothesis was based on the comparison between the eye position dependence during horizontal/vertical pursuit and yaw/pitch VOR. The VOR does not follow Listing's law or the half-angle rule (Angelaki et al., 2003; Crawford and Vilis, 1991; Misslich et al., 1994; Misslich and Hess, 2000). Thus, the neural hypothesis would predict smaller vertical motoneuron dependence on eye position during the yaw/pitch VOR as compared to horizontal/vertical pursuit eye movements. Again, the results were inconsistent with these predictions. Because none of the neural hypothesis predictions were supported by the data, we conclude that motoneurons do not carry the appropriate motor drive to generate the noncommutative-driven torsion during pursuit eye movements. Thus, our results demonstrate that motoneuron firing rates are not consistent with a neural coding of angular velocity, thus contradicting scheme 1 (Figure 1B). In contrast, our results support the notion that motoneurons encode the derivative of eye position and that the half-angle rule is implemented by the mechanical properties of the eyeball itself (schemes 2a and 2b). Yet, the present experiments were not designed to distinguish between schemes 2a (Raphan, 1998) and 2b (Smith and Crawford, 1998; Tweed et al., 1994), which differ in the premotor planning of eye movements (see section "Do Central Neural Networks Implement Noncommutative Computations?"). Neither can these experiments directly support nor contradict the pulley hypothesis (Demer et al., 2000; Kono et al., 2002).

Previous studies of ocular motoneuron properties only focused on describing the dynamics, recruitment

thresholds, and eye position sensitivities of cells in the abducens, trochlear, and oculomotor nuclei in relationship to either horizontal or vertical eye movements (De la Cruz et al., 1989; Delgado-Garcia et al., 1986; Fuchs and Luschei, 1970; Fuchs et al., 1988; Henn and Cohen, 1973; Henn et al., 1982; Hepp and Henn, 1985; Mays et al., 1991; Precht et al., 1979; Pastor et al., 1991; Robinson, 1970; Robinson and Keller, 1972; Schiller, 1970; Stahl and Simpson, 1995; Sylvestre and Cullen, 1999; Zhou and King, 1998). Only Suzuki et al. (1999) have characterized the static eye position properties of ocular motoneurons in three dimensions. The experiments reported here characterize motoneurons during dynamic stimuli optimized to address how three-dimensional rotations are implemented.

What Happens during the VOR?

How a mechanical solution potentially utilizing extraocular muscle pulleys can account for the three-dimensional eye orientation properties during pursuit and saccades has been previously quantified (Quaia and Optican, 1998). However, the pulley function during the VOR has remained uncertain. If extraocular muscle pulleys implement the half-angle rule by imposing an eye position-dependent pulling direction for the muscles, how is this property "undone" during the VOR? It was originally proposed that the pulleys might advance and retract along their muscle paths, adopting one arrangement for Listing's law and another for the VOR (Demer et al., 2000). This theory, however, has been shown to be incorrect (Misslich and Tweed, 2001). Using behavioral and computational arguments, several studies have recently shown that the three-dimensional eye orientation during the VOR requires a large neural contribution (Angelaki, 2003; Misslich and Tweed, 2001; Smith and Crawford, 1998). Demer and colleagues have reached a similar conclusion based on recent fMRI results regarding the pulley arrangement during ocular convergence and static counterrolling, conditions that result in a change in the orientation of Listing's plane (J.L. Demer and R.A. Clark, 2003, Soc. Neurosci., abstract; Demer et al., 2003). Yet, these ideas remain qualitative, and further work is necessary to understand how the brain controls three-dimensional eye orientation during the VOR, given a mechanical plant that might be optimized to exhibit an eye position-dependent pulling direction consistent with the half-angle rule.

Do Central Neural Networks Implement Noncommutative Computations?

Although the present results contradict the notion that motoneurons carry a neural signal to account for noncommutativity during pursuit, one should not conclude that these signals do not exist in the brain. Numerous studies have already illustrated that neural networks must incorporate noncommutative mathematics in the computation of the appropriate sensorimotor drive. For example, this important concept has been extensively demonstrated for the VOR (Angelaki, 2003; Misslich and Tweed, 2001; Misslich et al., 1994; Tweed et al., 1999), for head-free gaze shifts (Crawford and Vilis, 1991; Crawford and Guitton, 1997; Tweed, 1997), and for the visuomotor transformations from retinal information into kinematically correct gaze movements (Crawford and Guitton, 1997; Klier and Crawford, 1998; Klier et al., 2005; Medendorp et al., 2002). Furthermore, neurophysiological evidence for noncommutative signals has previously been provided for the premotor processing of pursuit eye movements (Angelaki and Dickman, 2003). Consistent with these experimental results, several modeling studies of sensorimotor transformations, which have incorporated muscle pulleys, must also utilize noncommutative computations in central neural networks (Smith and Crawford, 1998, 2005; Tweed et al., 1994, 1999). Thus, in light of the present results and those of previous studies supporting the existence of noncommutative operators in premotor brain circuits that deal with motor planning for eye movements, we conclude that scheme 2b (Figure 1B) is the one most consistent with all behavioral, modeling, and neurophysiological observations.

In conclusion, when considering the often-heated debates about noncommutativity, it is important to always consider the context in which these arguments are made. The present results during pursuit in head-fixed animals and initial eye positions in Listing's plane are inconsistent with an exclusively neural hypothesis for noncommutativity, suggesting that part of the solution for kinematically appropriate eye movements is found in the mechanical properties of the eyeball (Demer et al., 2000; Kono et al., 2002; Quaia and Optican, 1998). However, this result can only be thought of as a default mechanical solution that might simplify the generation of kinematically correct eye movements only in limited circumstances, e.g., for eye positions in Listing's plane and when considering a moving eye within a stationary head. As soon as the head is allowed to rotate, the noncommutativity problem is brought up again because of the geometry of head and body movements. How central neural networks deal with these complexities and how they generate the appropriate neural signals to control an eyeball, which is optimized for the implementation of the half-angle rule, during all eye and head movements remains to be investigated.

Experimental Procedures

Animals and Experimental Setup

Two juvenile fascicularis monkeys (*Maccaca fascicularis*) and one rhesus monkey (*Maccaca mulatta*) were chronically implanted with a head-restraint delrin ring and scleral coils to measure three-dimensional (3D) eye movements (cf. Angelaki, 2003; Angelaki et al., 2003). In addition, a removable delrin platform was stereotaxically placed near the skull and fitted inside the ring during each experiment. Extracellular recordings were obtained with epoxy-coated tungsten microelectrodes, inserted into 26 gauge guide tubes, advanced through a predrilled hole in the platform, and manipulated vertically with a remote control microdrive. The platforms had staggered rows of holes spaced 0.8 mm apart within a row, large enough to fit the 26 gauge guide tubes. Each platform could move in 0.4 mm steps, allowing for finer placement of electrode tracks. The platform was slanted relative to the sagital plane by 10° or 16°, to provide better access to the midline trochlear and oculomotor nuclei. All surgical procedures were performed under sterile conditions in accordance to institutional and NIH guidelines.

During experiments, the monkey was seated in a primate chair with its head positioned such that the horizontal stereotaxic plane

was aligned with the earth horizontal plane. The primate chair was then secured inside the inner frame of a vestibular turntable consisting of a three-dimensional rotator (Acutronics Inc, Pittsburg, PA). Eye movements were measured with a three-field magnetic search coil system (16 inch cube; CNC Engineering, Seattle, WA) that was attached to the inner gimbal of the turntable. Eye movements were recorded in three dimensions and calibrated daily during experiments with the animal fixating vertically and horizontally eccentric targets, as explained in detail elsewhere (Angelaki et al., 2003; Angelaki and Dickman, 2003; Klier et al., 2005). For each recording session, the eye coil signals, as well as velocity tachometer and position feedback signals from the rotators, were low-pass filtered (200 Hz, 6 pole Bessel), digitized at a rate of 833.33 Hz (Cambridge Electronics Design, model 1401 Plus, 16 bit resolution), and stored for offline analysis. Neural activity was amplified, filtered (300 Hz to 6 kHz), and passed through a BAK Instruments dual time-amplitude window discriminator. Single-unit spikes triggered acceptance pulses (BAK window discriminator) that were stored on a computer using the event channel of the 1401.

Animals were trained to fixate and pursue a small laser target that was back-projected onto a flat screen at a distance of 33 cm using a laser and x-y mirror galvanometer system (General Scanning), which was secured on the wall of the room. This system also provided a space-fixed target for the vestibulo-ocular reflex. An additional laser was mounted on top of the turntable and, because it moved with the animal, provided a head-fixed target during rotational motion for VOR cancellation tasks. During fixation at the ±20° eccentric positions, vergence angle changed little, as compared to fixation of straight-ahead targets (~4.5° versus 5.2°, respectively). The behavioral performance of the animal was continuously monitored using electronic behavioral windows, which ensured that eye position was maintained within 1.5° of ideal target fixation. This "eye-in-window" signal was monitored by the CED for online juice reward delivery and was saved for offline analyses. Behavioral windows for each eye were calculated online on the basis of the geometrical relationships that should govern appropriate target fixation or ideal target stabilization for a given motion of the target and/or head movement (Angelaki and Dickman, 2003).

Oculomotor and Trochlear Nuclei and Nerve Recordings

Electrode penetrations were focused in the rostral brainstem, aiming first at the trochlear (TR) and oculomotor (OC) nuclei and subsequently at the TR and OC nerve rootlets (containing axons innervating extraocular muscles). TR neurons were identified based on their characteristic burst-tonic activity with downward and abducting on-directions (Fuchs and Luschei, 1971; Hepp and Henn, 1985; Suzuki et al., 1999). The respective motoneuron pools in the OC nuclei were identified based on the characteristic burst-tonic activities with upward, downward, or horizontal on-directions. During penetrations through the OC nuclei, on-directions were segregated such that, within the same penetration, recording electrodes would sequentially go through patches of neuron pools (typically for less than 0.5 mm) with horizontal, upward, or downward preferred directions. As an additional anatomical landmark for our recording locations, we also mapped the rostral interstitial nucleus of the medial longitudinal fasciculus (riMLF) that contains short-lead vertical and torsional burst neurons (Vilis et al., 1989; Suzuki et al., 1995).

The neurons recorded within the TR and OC nuclei were not specifically identified as motoneurons. Thus, to verify that the described properties were indeed characteristic of ocular motoneurons, we also recorded from their respective rootlets. All fiber recordings had monophasic action potentials with a short duration, lasting less than 1 ms. OC nerve fibers were found below the riMLF, slightly anterior and ventral to the OC nuclei. Unlike the OC nuclei, during recordings from the OC rootlets we encountered horizontal, upward, and downward-preferred direction fibers intermingled. TR nerve fibers were recorded close to the decussation, as well as anterior and posterior to the decussation, 1–3 mm lateral from the midline (Suzuki et al., 1999). For these experiments, our goal was to characterize the activities of all motoneuron groups with vertical on-directions, but it was not necessary to identify the particular muscle each fiber innervated. Thus, with the only exception of TR fibers (innervating the superior oblique) that are anatomically segregated from the rest, no attempt was made to specifically identify inferior oblique, superior rectus, or inferior rectus cells or fibers.

Experimental Protocol

Our recordings concentrated mostly on vertical (TR and OC) motoneurons. As a control, we also recorded from medial rectus (MR) motoneurons using an identical experimental protocol (see below). Each cell was first tested to verify that there was no response modulation during sinusoidal horizontal (yaw) and vertical (pitch) rotations at 0.5 Hz, ±10° with the animal fixating a central, head fixed target that moved with the animal (i.e., VOR cancellation). In addition, the cell's static eye position sensitivity was evaluated by recording neural activities during fixation of targets with eccentricities extending ±10°, ±15°, ±20° horizontally and vertically.

The main experimental protocol was as follows.

Pursuit Protocol

A minimum of 20 cycles of 0.6 Hz (±5°) horizontal pursuit with the eyes at five to seven vertical positions (i.e., 0° [straight-ahead], ±10°, ±15°, and ±20°) in the midsagittal plane, as well as vertical pursuit at corresponding horizontal eccentricities (0°, ±10°, ±15°, and ±20°). These stimuli elicited eye velocity with a peak of ~20°/s.

VOR Protocol

A minimum of 20 cycles of 2 Hz (±1.2°) yaw rotation with the eyes at five to seven vertical positions (i.e., 0°, ±10°, ±15°, and ±20° up/down) in the midsagittal plane, as well as pitch rotation during fixation at 0°, ±10°, ±15°, and ±20° left/right in the horizontal plane. These stimuli elicited eye velocity with a peak of ~15–16°/s.

In addition to the main experimental protocol where eye position was varied in an orthogonal direction to target motion, a subpopulation of cells was also tested during horizontal and vertical pursuit at different horizontal and vertical eccentricities, respectively. This additional protocol served as a control, because in the latter condition where the eye only assumes secondary positions, no eye position-dependent torsion is evoked (Tweed and Vilis, 1987, 1990).

If satisfactory isolation was maintained, cell activity was then recorded during roll VOR (2 Hz, ±1.2°) while the monkey maintained fixation of a central target. Because testing for the roll VOR protocol required manual repositioning of the animal, cell isolation was often lost in the process. As a result, only a small subpopulation of cells (24) was tested during roll head movements. For all VOR protocols, two to five cycles with the target on (in a softly illuminated room) were intermingled with two to three cycles in complete darkness. Only the latter values were used for quantitative analyses.

Data Analyses

All data analyses were performed offline using Matlab. Three-dimensional eye positions were expressed as rotation vectors using straight-ahead as the reference position. Eye movements were expressed in a right-handed coordinate system with positive directions being clockwise, downward, or leftward from the subject viewpoint (Angelaki et al., 2003; Angelaki and Dickman, 2003). Primary position (i.e., the eye orientation perpendicular to Listing's plane) was within a few degrees ($\leq$4°) from straight-ahead, with the exception of one animal, where primary position was shifted 6.5° downward. Saccades and fast phases were identified and removed through a semiautomated computer algorithm based on a higher derivative of eye velocity. The algorithm offered manual inspection of the automatically detected fast phases and allowed the experimenter to correct potential misidentifications. For each recorded run, neural data, expressed as instantaneous firing rate, were also "desaccaded" using a window that extended from 50 ms before to 200 ms after each saccade.

To quantify neural firing rates during pursuit and the VOR, desaccaded neural activities from multiple stimulus cycles were folded in time into a single cycle instantaneous frequency response for each stimulus condition (e.g., Figures 2 and 3). Only portions in which eye positions were within ±1°–2° of the target have been included in the folding for further analyses. Both the evoked horizontal, vertical, and torsional components of eye velocity and the neural response during rotation and pursuit were quantified by fitting a sine function (first and second harmonic of the stimulus and a DC offset) to the overlaid data using a nonlinear least-squares

algorithm based on the Levenberg-Marquardt method (Angelaki and Dickman, 2003). Response gains were expressed as sp/s per deg/s of evoked eye velocity, by dividing peak-to-trough firing rate with peak-to-trough horizontal, vertical, or torsional eye velocity. Phase during pursuit was expressed as the difference (in degrees) between peak neural activity and peak eye velocity. For the VOR, cycles during target fixation and in complete darkness were analyzed separately. Positive directions for head motion were leftward, downward, and clockwise (from the animal's perspective). The static eye position sensitivity was evaluated using multiple linear regression analysis. Results were similar to those previously reported by other motoneuron studies (e.g., Fuchs and Luschei, 1970; Fuchs et al., 1988; Henn and Cohen, 1973; Sylvestre and Cullen, 1999; Suzuki et al., 1999), with all motoneurons characterized with burst-tonic activities, including both saccadic and tonic eye position sensitivities. In addition, care was taken that all motoneuron recordings were obtained from the center of the OC nuclei. Thus, although not directly identified as such, it is most likely that recorded motoneuron and fibers innervated twitch muscle fibers (Buttner-Ennever and Horn, 2002; Buttner-Ennever et al., 2001). In contrast, we had no way of distinguishing global and orbital layer motoneurons, since their relative location within the classical boundaries of the motor nuclei and potential differences in their physiological response properties have yet to be identified.

Computing the Predictions of the Neural Hypothesis

To quantitatively compare whether the observed motoneuron dependence on eye position supports or contradicts the neural hypothesis, a "predicted" slope was computed as follows. We assumed that the peak firing rate modulation of each vertical motoneuron during eccentric pursuit consists of two terms, one due to its sensitivity to vertical, *Sv* (in units of sp/s per °/s), and the other due to its sensitivity to torsional eye velocity, *St* (in units of sp/s per °/s). Thus, if *V* and *T* represent the respective vertical and torsional eye velocities generated, one can describe neural firing rate during vertical pursuit as follows:

$$\text{Firing rate} = V(Sv) \pm T(St)$$

After dividing by *V*, neural response *gain* during vertical pursuit (*Vgain*) can be described as

$$Vgain = Sv \pm St(T/V)$$

Because, as shown in the Results, the ratio *T*/*V* depends linearly on eye position, *E* [i.e., $(T/V) = aE + m$, where *a* and *m* are parameters that can be computed for each animal, see Figures 5C and 5D], the equation can be rewritten as

$$Vgain = Sv + m(St) \pm (a(St))E \quad (1a)$$

Similarly for horizontal pursuit gain [where $(T/H) = aE + m'$],

$$Hgain = Sh + m'(St) \pm (a(St))E \quad (1b)$$

Equations 1a and 1b illustrate that the slope of neural pursuit gain as a function of eye position (predicted by the neural hypothesis) can be easily estimated if torsional sensitivity, *St*, is known (since the eye velocity ratio slope, *a*, is easily computed for each animal, e.g., Figures 4A and 4B). A lower bound for *St* can be computed as $St \cong Sv$, the cell's sensitivity to vertical eye velocity, computed during vertical pursuit at zero horizontal eccentricity. This approximation is consistent with the on-direction of vertical motoneurons (Suzuki et al., 1999). The torsional eye velocity sensitivity could be more directly estimated for motoneurons that were tested during roll head movements (Figure 2C). The predictions according to Equations 1a and 1b assume similar response dynamics for the vertical and torsional sensitivity contributions, an assumption supported by the data (Figure 2D).

Neural response gains during horizontal or vertical pursuit (and yaw/pitch VOR) were plotted as a function of the respective eye position, and these relationships were quantified using first-, second-, and third-order polynomials. Because either no or only a minor improvement in the fit was noticed with the higher models, the data presented here refer to the slope (and associated p value of the fit) of the linear model. To directly compare neural behavior with the predicted values, we also *simultaneously* fitted the horizontal and vertical pursuit dependence of each cell on eye position using three (rather than four) parameters, as follows: vertical pursuit responses for each cell were fitted by the equation $y_{vertical\ pursuit} = ax + b_1$, whereas horizontal pursuit responses were fitted with the equation $y_{horizontal\ pursuit} = \pm ax + b_2$ (where all three parameters, *a*, b_1, and b_2 were unconstrained and allowed to assume either positive or negative values). Whether horizontal pursuit slopes were the same ("+" in $y_{horizontal\ pursuit}$) or opposite ("–" in $y_{horizontal\ pursuit}$) from those during vertical pursuit depended on the motoneuron's horizontal and vertical on-directions: motoneurons with left/up and right/down on-directions had similar sign slopes for horizontal and vertical pursuit. Motoneurons with left/down and right/up on-directions had opposite sign slopes for horizontal and vertical pursuit (Table 1; this particular pattern of predictions depends on the coordinate system used to express eye movements).

This three-parameter model that was simultaneously fitted to both horizontal and vertical pursuit data for each cell was used to estimate the neural firing rate slope, *a*, that was then directly compared with the predictions of the neural hypothesis. Table 1 presents a lookup table of the expected sign of the eye position slope of neural firing rates during horizontal and vertical pursuit, according to their respective on-directions.

Acknowledgments

The work was supported by NIH grants R01 EY12814 and R01-EY15271. We would like to thank Nuo Li for help with data analyses and Greg DeAngelis, David Dickman, and the members of our lab for comments on the manuscript.

Received: April 7, 2005
Revised: May 9, 2005
Accepted: May 26, 2005
Published: July 20, 2005

References

Angelaki, D.E. (2003). Three-dimensional ocular kinematics during combined rotational and translational motion: evidence for functional rather than mechanical constraints. J. Neurophysiol. *89*, 2685–2696.

Angelaki, D.E., and Dickman, J.D. (2003). Premotor neurons encode torsional eye velocity during smooth pursuit eye movements. J. Neurosci. *23*, 2971–2979.

Angelaki, D.E., and Hess, B.J.M. (2004). Control of eye orientation: Where does the brain's role end and the muscle's begin? Eur. J. Neurosci. *19*, 1–10.

Angelaki, D.E., Zhou, H.H., and Wei, M. (2003). Foveal vs. full-field visual stabilization strategies for translational and rotational head movements. J. Neurosci. *23*, 1104–1108.

Buttner-Ennever, J.A., and Horn, A.K. (2002). The neuroanatomical basis of oculomotor disorders: the dual motor control of extraocular muscles and its possible role in proprioception. Curr. Opin. Neurol. *15*, 35–43.

Buttner-Ennever, J.A., Horn, A.K., Scherberger, H., and D'Ascanio, P. (2001). Motoneurons of twitch and nontwitch extraocular muscle fibers in the abducens, trochlear, and oculomotor nuclei of monkeys. J. Comp. Neurol. *438*, 318–335.

Cannon, S.C., and Robinson, D.A. (1987). Loss of the neural integrator of the oculomotor system from brain stem lesions in monkey. J. Neurophysiol. *57*, 1383–1409.

Crawford, J.D., and Guitton, D. (1997). Visual-motor transformations required for accurate and kinematically correct saccades. J. Neurophysiol. *78*, 1447–1467.

Crawford, J.D., and Vilis, T. (1991). Axes of rotation and Listing's law during rotations of the head. J. Neurophysiol. *65*, 407–423.

Crawford, J.D., Martinez-Trujillo, J.C., and Klier, E.M. (2003). Neural control of three dimensional eye and head movements. Curr. Opin. Neurobiol. *13*, 655–662.

De la Cruz, R.R., Escudero, M., and Delgado-Garcia, J.M. (1989).

Behaviour of medial rectus motoneurons in the alert cat. Eur. J. Neurosci. *1*, 288–295.

Delgado-Garcia, J.M., Del Pozo, F., and Baker, R. (1986). Behavior of neurons in the abducens nucleus of the alert cat. I. Motoneurons. Neuroscience *17*, 929–952.

Demer, J.L., Miller, J.M., Poukens, V., Vinters, H.V., and Glasgow, B.J. (1995). Evidence for fibromuscular pulleys of the recti extraocular muscles. Invest. Ophthalmol. Vis. Sci. *36*, 1125–1136.

Demer, J.L., Oh, S.Y., and Poukens, V. (2000). Evidence for active control of rectus extraocular muscle pulleys. Invest. Ophthalmol. Vis. Sci. *41*, 1280–1290.

Demer, J.L., Kono, R., and Wright, W. (2003). Magnetic resonance imaging of human extraocular muscles in convergence. J. Neurophysiol. *89*, 2072–2085.

Dimitrova, D.M., Shall, M.S., and Goldberg, S.J. (2003). Stimulation-evoked eye movements with and without the lateral rectus muscle pulley. J. Neurophysiol. *90*, 3809–3815.

Ferman, L., Collewijn, H., and Van Den Berg, A.V. (1987). A direct test of Listing's Law: I. Human ocular torsion measured in static tertiary positions. Vision Res. *27*, 929–938.

Fuchs, A.F., and Luschei, E.S. (1970). Firing patterns of abducens neurons of alert monkeys in relationship to horizontal eye movement. J. Neurophysiol. *33*, 382–392.

Fuchs, A.F., and Luschei, E.S. (1971). The activity of single trochlear nerve fibers during eye movements in the alert monkey. Exp. Brain Res. *13*, 78–89.

Fuchs, A.F., Scudder, C.A., and Kaneko, C.R.S. (1988). Discharge patterns and recruitment order of identified motoneurons and internuclear neurons in the monkey abducens nucleus. J. Neurophysiol. *60*, 1874–1895.

Goldberg, S.J., and Shall, M.S. (1999). Motor units of extraocular muscles: Recent findings. Prog. Brain Res. *123*, 221–232.

Goldberg, S.J., Meredith, M.A., and Shall, M.S. (1998). Extraocular motor unit and whole-muscle responses in the lateral rectus muscle of the squirrel monkey. J. Neurosci. *18*, 10629–10639.

Goldstein, H. (1980). Classical Mechanics (Reading, MA: Addison-Wesley Publishing Company).

Haslwanter, T. (1995). Mathematics of three-dimensional eye rotations. Vision Res. *35*, 1727–1739.

Haslwanter, T. (2002). Mechanics of eye movement: implications of the "orbital revolution". Ann. N Y Acad. Sci. *956*, 33–41.

Haslwanter, T., Straumann, D., Hepp, K., Hess, B.J., and Henn, V. (1991). Smooth pursuit eye movements obey Listing's Law in the monkey. Exp. Brain Res. *87*, 470–472.

von Helmholtz, H. (1867). Handbuch der Physiologischen Optik (Hamburg: Voss).

Henn, V., and Cohen, B. (1973). Quantitative analysis of activity in eye muscle motoneurons during saccadic eye movement and positions of fixation. J. Neurophysiol. *36*, 115–126.

Henn, V., Buttner-Ennever, J.A., and Hepp, K. (1982). The primate oculomotor system. Hum. Neurobiol. *1*, 77–85.

Hepp, K., and Henn, V. (1985). Iso-frequency curves of oculomotor neurons in the rhesus monkey. Vision Res. *25*, 493–499.

Klier, E.M., and Crawford, J.D. (1998). Human oculomotor system accounts for 3-D eye orientation in the visual-motor transformation for saccades. J. Neurophysiol. *80*, 2274–2294.

Klier, E.M., Angelaki, D.E., and Hess, B.J. (2005). The roles of gravitational cues and efference copy signals in the rotational updating of memory saccades. J. Neurophysiol. in press.

Kono, R., Clark, R.A., and Demer, J.L. (2002). Active pulleys: magnetic resonance imaging of rectus muscle paths in tertiary gazes. Invest. Ophthalmol. Vis. Sci. *43*, 2179–2188.

Mays, L.E., Zhang, Y., Thorstad, M.H., and Gamlin, P.D. (1991). Trochlear unit activity during ocular convergence. J. Neurophysiol. *65*, 1484–1497.

Medendorp, W.P., Van Gisbergen, J.A.M., and Gielen, C.C.A.M. (2002). Human gaze stabilization during active head translations. J. Neurophysiol. *87*, 295–304.

Miller, J.M., and Robins, D. (1992). Extraocular muscle forces in alert monkey. Vision Res. *32*, 1099–1113.

Miller, J.M., Demer, J.L., and Rosenbaum, A.L. (1993). Effect of transposition surgery on rectus muscle paths by magnetic resonance imaging. Ophthalmology *100*, 475–487.

Misslich, H., and Hess, B.J. (2000). Three-dimensional vestibulo-ocular reflex of the monkey: optimal retinal image-stabilization versus listing's law. J. Neurophysiol. *83*, 3264–3276.

Misslich, H., and Tweed, D. (2001). Neural and mechanical factors in eye control. J. Neurophysiol. *86*, 1877–1883.

Misslich, H., Tweed, D., Fetter, M., Sievering, D., and Koenig, E. (1994). Rotational kinematics of the human vestibuloocular reflex. III. Listing's Law. J. Neurophysiol. *72*, 2490–2502.

Pastor, A.M., Torres, B., Delgado-Garcia, J.M., and Baker, R. (1991). Discharge characteristics of medial rectus and abducens motoneurons in the goldfish. J. Neurophysiol. *66*, 2125–2140.

Porrill, J., Warren, P.A., and Dean, P. (2000). A simple control law generates Listing's positions in a detailed model of the extraocular muscle system. Vision Res. *40*, 3743–3758.

Precht, W., Anderson, J.H., and Blanks, R.H. (1979). Canal-otolith convergence on cat ocular motoneurons. Prog. Brain Res. *50*, 459–468.

Quaia, C., and Optican, L.M. (1998). Commutative saccadic generator is sufficient to control a 3-D ocular plant with pulleys. J. Neurophysiol. *79*, 3197–3215.

Quaia, C., and Optican, L.M. (2003). Dynamic eye plant models and the control of eye movements. Strabismus *11*, 17–31.

Raphan, T. (1998). Modeling control of eye orientation in three dimensions. I. Role of muscle pulleys in determining saccadic trajectory. J. Neurophysiol. *79*, 2653–2667.

Robinson, D.A. (1970). Oculomotor unit behavior in the monkey. J. Neurophysiol. *33*, 393–403.

Robinson, D.A., and Keller, E.L. (1972). The behavior of eye movement motoneurons in the alert monkey. Bibl. Ophthalmol. *82*, 7–16.

Schiller, P.H. (1970). The discharge characteristics of single units in the oculomotor and abducens nuclei of the unanesthetized monkey. Exp. Brain Res. *10*, 347–362.

Skavenski, A.A., and Robinson, D.A. (1973). Role of abducens neurons in vestibuloocular reflex. J. Neurophysiol. *36*, 724–738.

Smith, M.A., and Crawford, J.D. (1998). Neural control of rotational kinematics within realistic vestibuloocular coordinate systems. J. Neurophysiol. *80*, 2295–2315.

Smith, M.A., and Crawford, J.D. (2005). Distributed population mechanism for the 3-d oculomotor reference frame transformation. J. Neurophysiol. *93*, 1742–1761.

Stahl, J.S., and Simpson, J.I. (1995). Dynamics of abducens nucleus neurons and the influence of the flocculus. J. Neurophysiol. *73*, 1383–1395.

Suzuki, Y., Buttner-Ennever, J.A., Straumann, D., Hepp, K., Hess, B.J., and Henn, V. (1995). Deficits in torsional and vertical rapid eye movements and shift of Listing's plane after uni- and bilateral lesions of the rostral interstitial nucleus of the medial longitudinal fasciculus. Exp. Brain Res. *106*, 215–232.

Suzuki, Y., Straumann, D., Simpson, J.I., Hepp, K., Hess, B.J., and Henn, V. (1999). Three-dimensional extraocular motoneuron innervation in the rhesus monkey. I: Muscle rotation axes and on-directions during fixation. Exp. Brain Res. *126*, 187–199.

Sylvestre, P.A., and Cullen, K.E. (1999). Quantitative analysis of abducens neuron discharge dynamics during saccadic and slow eye movements. J. Neurophysiol. *82*, 2612–2632.

Tweed, D. (1997). Velocity-to-position transformation in the VOR and the saccadic system. In Three-Dimensional Kinematics of Eye, Head, and Limb Movements, M. Fetter, T. Haslwanter, H. Misslich, and D. Tweed, eds. (The Netherlands: Harwood Academic), pp. 375–386.

Tweed, D., and Vilis, T. (1987). Implications of rotational kinematics for the oculomotor system in three dimensions. J. Neurophysiol. *58*, 832–849.

Tweed, D., and Vilis, T. (1990). Geometric relations of eye position and velocity vectors during saccades. Vision Res. *30*, 111–127.

Tweed, D., Fetter, M., Andreadaki, S., Koenig, E., and Dichgans, J. (1992). Three-dimensional properties of human pursuit eye movements. Vision Res. *32*, 1225–1238.

Tweed, D., Misslisch, H., and Fetter, M. (1994). Testing models of the oculomotor velocity-to-position transformation. J. Neurophysiol. *72*, 1425–1429.

Tweed, D., Haslwanter, T., Happe, V., and Fetter, M. (1999). Noncommutativity in the brain. Nature *399*, 261–263.

Vilis, T., Hepp, K., Schwarz, U., and Henn, V. (1989). On the generation of vertical and torsional rapid eye movements in the monkey. Exp. Brain Res. *77*, 1–11.

Westheimer, G. (1957). Kinematics of the eye. J. Opt. Soc. Am. *47*, 967–974.

Zhou, W., and King, W.M. (1998). Premotor commands encode monocular eye movements. Nature *393*, 692–695.